Measuring the Newtonian constant of gravitation with a differential free-fall gradiometer: A feasibility study

Christian Rothleitner and Olivier Francis

Articles you may be interested in
Acoustic measurements of bouncing balls and the determination of gravitational acceleration
Phys. Teach. **51**, 312 (2013); 10.1119/1.4801369

Simultaneous measurement of gravity acceleration and gravity gradient with an atom interferometer
Appl. Phys. Lett. **101**, 114106 (2012); 10.1063/1.4751112

A superconducting gravity gradiometer for measurements from a moving vehicle
Rev. Sci. Instrum. **82**, 094501 (2011); 10.1063/1.3632114

Long term plumb-line alignment of precise measuring instruments: An adaptive digital controller designed for an autoleveling platform
Rev. Sci. Instrum. **81**, 105108 (2010); 10.1063/1.3492193

Direct ultrasonic measurement of solid propellant ballistics
Rev. Sci. Instrum. **70**, 4416 (1999); 10.1063/1.1150087

Measuring the Newtonian constant of gravitation with a differential free-fall gradiometer: A feasibility study

Christian Rothleitner[a] and Olivier Francis[b]

Faculty of Sciences, Technology and Communication, University of Luxembourg, Luxembourg

An original setup is presented to measure the Newtonian Constant of Gravitation G. It is based on the same principle as used in ballistic absolute gravimeters. The differential acceleration of three simultaneously freely falling test masses is measured in order to determine G. In this paper, a description of the experimental setup is presented. A detailed uncertainty budget estimates the relative uncertainty to be of the order of 5.3×10^{-4}, however with some improvements a relative uncertainty in G of one part in 10^4 could be feasible. © *2014 AIP Publishing LLC*. [http://dx.doi.org/10.1063/1.4869875]

I. INTRODUCTION

Since the first measurement of the gravitational constant in 1798, by Henry Cavendish,[1] nearly three hundred measurements have been performed. Although this is a relatively high number of measurements of a fundamental physical constant, the improvement in its relative uncertainty is quite poor. While Cavendish obtained a relative uncertainty of 7410 ppm, the best measurement ever done is of "only" 14 ppm.[2] However, this is not the sole issue regarding the measurements of the gravitational constant. There is also the problem that between different measurement results there are offsets by several standard deviations. This means obviously that at least one of the published results contains a systematic error. This wide spread of G-values lead even the Task Group on Fundamental Constants (CODATA) to increase the uncertainty of the recommended value from 126 ppm in 1986 to 1500 ppm in 1998, an action which was unique in the history of CODATA. An argument for CODATA was a publication of Kuroda, who showed that the time of swing of a torsion pendulum (the method which was used for most of all G-measurements) could be biased by a material property of the suspending wire; a fact which was so far excluded. In 2006, Schlamminger *et al.*[3] were able to measure G with a comparable precision as Gundlach and Merkowitz.[2] Their method was completely different from foregoing experiments. They used a beam balance, while Gundlach and Merkowitz[2] used a sophisticated torsion balance experiment. Fortunately both measured values agree with their standard uncertainties. In 2010, however, Parks and Faller[4] published their results of G, obtained by means of a pendulum setup. The determination was precise to 21 ppm, i.e., comparable to the best measurements ever done. They let six years pass before publishing their results. The reason was that their result differs by 10 standard deviations from the result of Gundlach and Merkowitz.[2] To date the reason for this discrepancy is still a miracle.[5] Nevertheless it shows

that no experiment is perfect. It is always possible to overlook some systematic effect. One way to uncover such effect is to make another experiment, based on a different measurement principle.

Here we present a setup to determine the Gravitational Constant, G, by means of a free-fall experiment. The idea is based on a former experiment where a free-fall absolute gravimeter *FG*5, from Micro-g LaCoste[6] Inc., was used.[7,8] The reported uncertainty of Schwarz *et al.*[8] was 1410 ppm. The main uncertainty sources were the changing environmental conditions, since this experiment measured the absolute value of the acceleration due to gravity, g. In order to eliminate the biggest uncertainties the source masses were changed in position; this gave a differential character to the experiment. In 2008, Lamporesi *et al.*[9] presented a quite similar experiment, though using atom interferometry rather than laser interferometry. Another difference to Schwarz *et al.* was that they used two test masses, rather than one. The measurement was then a measurement of the gradient, not of the absolute value of g. This is the differential measurement of Schwarz *et al.*,[8] but performed in one single measurement. The reported result shows an uncertainty of 1800 ppm. The measurement requires a precise knowledge of the local vertical gravity gradient. In order to reduce this uncertainty, the source masses have been changed in position as in Schwarz *et al.*[8] This movement unfortunately increased the uncertainty by producing tilts in the setup. Our setup is a further development of the described free-fall experiments. We drop macroscopic test masses, such as Schwarz *et al.*[8] and measure with a laser interferometer its trajectory under the influence of a big source mass, however the measurement principle is differential. We also do not drop only one test mass, but three at a time, separated vertically in space. The result is a measurement of the second vertical derivative of g. Such a setup makes, in principle, a change of the sources masses position unnecessary.

In the first part of this paper we describe the setup and some physical properties. In the second part, we provide a detailed uncertainty budget, before we give a summary and outlook in the conclusion part. As the Appendix we present a method to find the optimum position of the test mass with respect to the source masses.

---
[a]Present address: Physikalisch-Technische Bundesanstalt (PTB), Braunschweig, Germany; Electronic mail: christian.rothleitner@ptb.de
[b]Electronic mail: olivier.francis@uni.lu

85, 044501-1

II. THE INTERFEROMETER SETUP AND PRINCIPLE OF MEASUREMENT

The proposed instrument is based on the principle of a free-fall absolute gravimeter[10,11] (FFAG). In such a FFAG, a test mass, which contains a corner cube reflector, is released in a vacuum vessel. Its trajectory as function of free-fall time is measured by means of a Mach-Zehnder type laser interferometer. In order to enable a repetition of the measurement, the test mass is placed into an elevator. This elevator is accelerated with more than the local acceleration due to gravity – consequently the test mass hovers from the elevator and falls freely – and later decelerates in order to catch the test mass softly.

In order to explain the final design of our instrument let us first consider a modification of the FFAG, which basically measures the first derivative of g.

Fig. 1 is a sketch of a gradiometer which is simply derived by replacing the inertial isolated reference retroreflector in a Mach-Zehnder type interferometer of the FFAG by a second freely falling test mass. Both test masses ($CC_{1,2}$) in that design are assumed to be placed in the same elevator. The beam splitter (BS) is placed between both CCs and physically attached to the surrounding vacuum chamber. A laser light incident on BS is split into two beams. The first one passes the BS straight through; the second one is reflected by both CCs before recombining again with the beam of the first path at BS. A resulting fringe signal will be detected by means of a photo detector (Det). Both CCs will at the same time fall freely inside the vacuum chamber. For a constant acceleration, i.e., when zero vertical gravity gradient is assumed, both CCs would accelerate by the same amount due to earth's attraction. Their relative distance would not change and the interference frequency is constant. However, if there is a vertical gravity gradient present, the gravity g_1 which acts on the upper CC_1 is weaker (gravity decrease with increasing distance to Earth's center) than g_2, which acts on the lower CC_2. As a result, we observe a relative increase of the distance between both CCs during their free-fall. For Earth's gravity field the vertical gradient is about -0.3086 mGal m^{-1}. With such a setup we are not able to measure the absolute values of the acceleration due to gravity $g_{1,2}$ any more, but the differential acceleration, or the gradient $\gamma = (g_2 - g_1)/d$, where d denotes the separation between CC_1 and CC_2. We are able now to measure in a direct way the first derivative of the (vertical) gravity (or the second derivative of the gravity potential). From a different point of view we can say that we combined two FFAGs with a common reference mirror (see Fig. 1). Both gravimeters measure at different heights, but simultaneously and along the same plumb line.

Now we can go a step further and place two gradiometers along the same plumb line. We take simultaneous measurements with both gradiometers. Then we calculate the difference between the upper and the lower ones. The difference is the second derivative of g, or the third derivative of the potential V. In Fig. 2, this idea is sketched. A laser light is split into two beams by a first BS. Each beam is now the measurement beam for the upper and the lower gradiometer, respectively. After both beams have passed through the gradiometers, they are recombined by a further beam splitter before the signal is detected by a photo detector. The combination of two vertically aligned gradiometers includes a merging of the lower test mass (containing CC_2) of the upper gradiometer with the upper test mass (containing CC_3) of the lower gradiometer. As a result we have three freely falling test masses (CC_1, $CC_{2,3}$, and CC_4); all of them sit in the same elevator ensuring simultaneous free-falls. Again, the beam splitters of the gradiometers are rigid, and do not move with the elevator. If the gradient is assumed to be a constant and we assume the distance between CC_1 and $CC_{2,3}$ the same as between $CC_{2,3}$ and
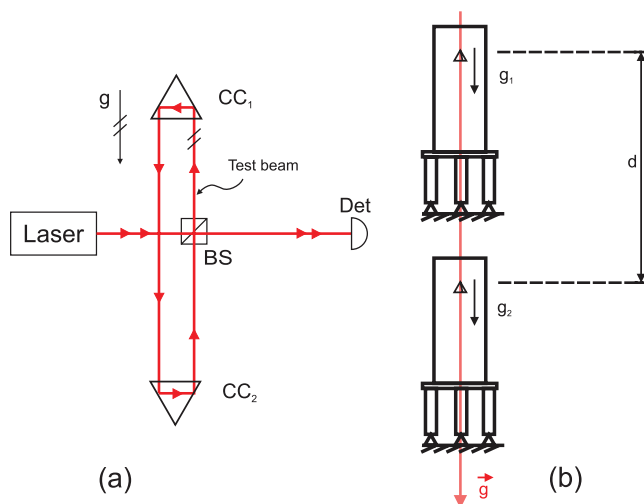

FIG. 1. (a) Gradiometer design. The reference mirror is replaced by a second freely falling retroreflector. BS – beam splitter, CC_i – corner cube retroreflector, Det – detector. The principle is sketched in figure (b): The gradiometer can be considered as two gravimeters measuring at the same time at different heights along the same plumb line. Since due to the vertical gravity gradient at different heights we have different gravity values, the difference in the measured values, divided by the height difference d of the gravimeters, gives the gradient.
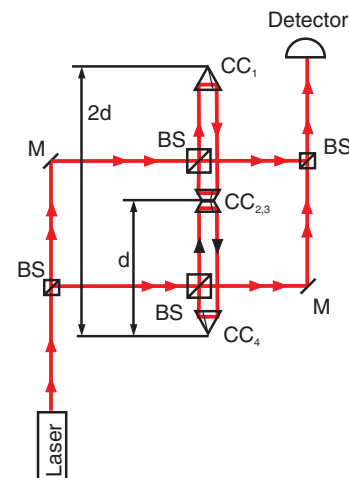
FIG. 2. Principle of the differential free-fall gradiometer. It can be considered as a combination of two gradiometers, or four gravimeters with a common reference mirror. M – mirror, BS – beam splitter, CC_i – corner cube retroreflectors. If the middle test mass is centered between the upper and the lower test mass and the gravity field is constant or linear, no path length change results between the upper and the lower gradiometer.

CC$_4$, the path length change in the upper gradiometer is the same as in the lower one and thus no fringe signal will appear. Only nonlinear gravity field strengths can be measured. The measured quantity is the second derivative of g, i.e.,

$$\gamma' := \frac{\partial \gamma}{\partial z} = \frac{\partial^2 g}{\partial z^2} = \frac{g_1 - 2g_{2,3} + g_4}{d^2} , \qquad (1)$$

where g_i ($i = 1,2,3,4$) refers to the gravity at the position of CC$_i$. With such a differential gradiometer we hence are insensitive to the absolute (background) field g and its first derivative, i.e., the vertical gravity gradient γ. A better signal to noise ratio is thus expected for local gravity anomalies. This property will be exploited for the G measurement.

It is interesting to note the following property of the instrument. It can be shown[12] that inertial forces can be separated from gravitational forces, when higher order gradients are measured. The measured force in a non-inertial system can be written as

$$\ddot{x}_k = f_k - 2a_{ik}\dot{a}_{ij}\dot{x}_j - a_{ik}\ddot{a}_{ij}x_j - \ddot{b}_k , \qquad (2)$$

where f_i denotes a gravitational force, derived from a potential $f_i = \partial V / \partial x_i$, a_{ik} denotes a rotation matrix, describing the relative rotation between an inertial frame and the non-inertial frame, and $\ddot{b}_k$ denotes the relative acceleration between both frames. The second term in (2) can be identified as the Coriolis force, the third term can be shown to contain the Euler and the centrifugal force. Differentiating twice with respect to x_i gives

$$\frac{\partial^2 \ddot{x}_i}{\partial x_i^2} = \frac{\partial^2 f_i}{\partial x_i^2} = -\frac{\partial^3 V}{\partial x_i^3}, \qquad (3)$$

i.e., all inertial forces disappear and we are left with only the third derivative of the gravitational potential. As a consequence the second derivative of the measured acceleration is purely of gravitational origin. This is consistent with Einstein's equivalence principle. The reason lies in the property of inertial forces. They do not create tidal forces as gravitation does. In general relativity, hence, inertial forces result in a vanishing Riemann tensor, i.e., inertial forces do not curve space.

III. UNCERTAINTY ANALYSIS

The relative uncertainty of the CODATA value[13] for Newton's Gravitational Constant G is 1.2×10^{-4}. In order to conduct a G measurement with the proposed instrument with this uncertainty or better, the alignment and quality of optical parts must meet certain requirements. In this section, we discuss them in detail.

Since the differential free-fall gradiometer is based on the same measurement principle as a common free-fall absolute gravimeter (it can be considered as a combination of four free-fall absolute gravimeters), we can apply the same analysis made for those instruments (see Ref. 10 and 11).

A. Expected gravity signal

The interferometer design, as well as the possible positions of the external source masses, are shown in the following Figure 3 (for labels see Table I).
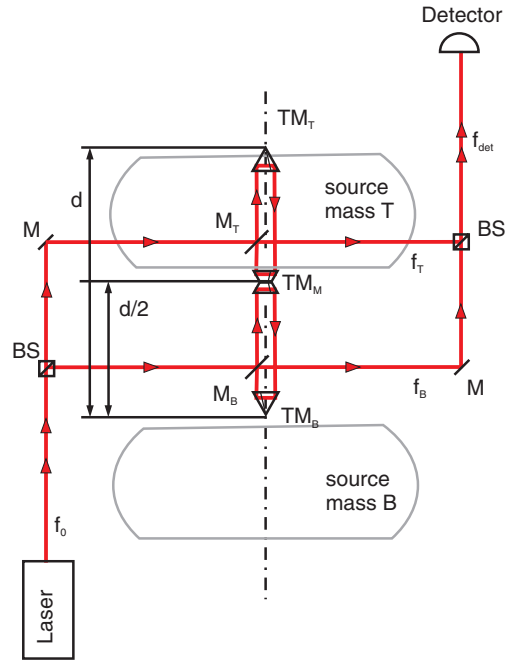

FIG. 3. Interferometer design of the differential free-fall gradiometer with one possibility of positioning the external source masses are depicted. (For labels see Table I).

If test masses TM_T and TM_M fall freely, then the laser frequency f_T in the top gradiometer will be shifted and will be

$$f_T = f_0 - \Delta f_M - \Delta f_T \qquad (4)$$

after leaving the gradiometer. The minus sign of Δf_M occurs because TM_M is departing from mirror M_T, hence the frequency decreases. For TM_T the frequency has to increase. For the bottom gradiometer we get, respectively,

$$f_B = f_0 + \Delta f_M - \Delta f_B, \qquad (5)$$

when test masses TM_M and TM_B are dropped. The detected frequency f_{det} is then the beat frequency between the top and bottom frequency

$$\begin{aligned}
\Delta f_{det} &= f_B - f_T \\
&= f_0 + \Delta f_M - \Delta f_B - (f_0 - \Delta f_M - \Delta f_T) \\
&= 2\Delta f_M - (\Delta f_B + \Delta f_T). \qquad (6)
\end{aligned}$$

As we are only interested in the relative motion of the test masses, we can transform into a system, where $\Delta f_M = 0$, i.e., we are comoving with TM_M. With the transformation

$$\Delta \tilde{f}_B = \Delta f_B - \Delta f_M, \qquad (7)$$

TABLE I. Labels used in Figure 3.

TM_T	Top test mass
TM_M	Middle test mass
TM_B	Bottom test mass
f_{det}	Detected frequency
f_T	Frequency in top gradiometer
f_B	Frequency in bottom gradiometer
f_0	Laser frequency in laboratory frame

$$\Delta \tilde{f}_T = \Delta f_T - \Delta f_M, \qquad (8)$$

we obtain for constant velocities

$$\Delta f_{det} = -(\Delta \tilde{f}_B + \Delta \tilde{f}_T) = -\left(\frac{2\tilde{v}_B}{c}f_0 + \frac{2\tilde{v}_T}{c}f_0\right)$$

$$= -\frac{2f_0}{c}(\tilde{v}_B - \tilde{v}_T). \qquad (9)$$

Here we used the first-order Doppler shift

$$\Delta f_0 = \frac{2v}{c}f_0 = \frac{2v}{\lambda_0}. \qquad (10)$$

With

$$\frac{\lambda_0}{2}\int_0^T \Delta f_0 dt = \Delta z, \qquad (11)$$

we get

$$\Delta z = \frac{\lambda_0}{2}\int_0^T \Delta f_{det} dt$$

$$= -\frac{\lambda_0}{2}\left[\int_0^T \Delta \tilde{f}_B dt + \int_0^T \Delta \tilde{f}_T dt\right]$$

$$= -T(\tilde{v}_B - \tilde{v}_T). \qquad (12)$$

For an accelerated motion we would get

$$\Delta z = -\left[\int_0^T (v_{\tilde{B},0} + \tilde{g}_B t)dt + \int_0^T (v_{\tilde{T},0} + \tilde{g}_T t)dt\right]$$

$$= -(v_{\tilde{B},0} + v_{\tilde{T},0})T - \frac{(\tilde{g}_B + \tilde{g}_T)}{2}T^2. \qquad (13)$$

Equation (13) can likewise be expressed in the laboratory frame as

$$\Delta z = -\left[\int_0^T (v_{B,0} + g_B t)dt + \int_0^T (v_{T,0} + g_T t)dt\right.$$

$$\left. - 2\int_0^T (v_{M,0} + g_M t)dt\right]$$

$$= -(v_{B,0} - 2v_{M,0} + v_{T,0})T$$

$$- \frac{(g_B - 2g_M + g_T)}{2}T^2. \qquad (14)$$

Equations (13) and (14) describe the differential change in separation of test masses TM_B and TM_M, with respect to TM_T and TM_M, which is a function of the differential acceleration g_{diff} and velocity v_{diff} of all three test masses

$$\Delta z = -(v_{diff})T - \frac{(g_{diff})}{2}T^2. \qquad (15)$$

By analysing Δz we thus obtain the differential acceleration. This analysis, however, is the same as in the gravimeter. We do not have to consider any multipass for the interferometer, that is, when considering two zerocrossings (rising to falling edge, or vice versa) the separation between the test masses has changed by $\lambda/4$. It follows that the software used for the gravimeter can be directly applied to obtain the differential acceleration; no modifications need to be done.

A calculation of the peak field strength produced by tungsten cylinders, such as used by Schwarz et al.,[7,8] give 27 μGal (5 cylinders with a diameter of about 16.6 cm and a height of about 10.4 cm and a mass of 39.7 kg each, in a torus-like arrangement). Assume that one torus of 5 cylinders were placed as the source mass T in Figure 3. If perfectly placed, the field strength due to the source masses at position TM_T and TM_M would be +27 and −27 μGal, respectively. If we further assume that the gravity field of the source mass decays very rapidly with vertical distance, so that at position TM_B its value is zero, the measured differential gravity g_{diff} must be (in μGal)

$$g_{diff} = \Delta^2 g = (g_B - 2g_M + g_T)$$

$$= (0 - 2 \times 27 + (-27))$$

$$= -81. \qquad (16)$$

Here we neglected the initial velocities and assumed the gravity values to be constant over the drop lengths. Since the gravity due to the source mass at position TM_B is usually not zero, the net differential gravity should be less than 81 μGal. If two tori, of 5 cylinders each, were arranged as in Figure 3, that is, we have two source masses (T and B), then the net differential gravity could be at the most $4 \times 27\,\mu$Gal $= 108\,\mu$Gal (absolute value). The true value is different, since the gravity values at positions TM_T, TM_M, and TM_B are not 27 μGal any more, for the gravity field, produced by the upper torus, can partly compensate the gravity field, produced by the lower torus.

B. Differential mode uncertainties

1. Beam verticality, beam diffraction, and beam shear for Gaussian beams

In a free-fall gravimeter, the laser beam must be well aligned along the verticality, since the test mass moves along this line. An imperfect alignment leads to the so-called cosine error, which is well known for laser-interferometric measurements. However, this error is often given under the assumption that the laser beam consists of plane waves, which leads to an overestimated error. Cavagnero et al.[14] gave a general description of errors arising from diffraction effects, caused by the Gaussian shape of the beam profile in laser interferometers. This thorough analysis includes the diffraction effect due to Gaussian beam propagation, the cosine error (here: beam verticality) for a Gaussian beam and finally the error due to beam shear. Beam shear is in fact not a common mode effect and will be treated later, however we will give the complete expression for the excess phase to the plane wave approximation, which is

$$\frac{\Delta \lambda}{\lambda} = \frac{\left(1 - \frac{x_0^2}{2\omega_0^2}\right)\theta^2}{4} + \frac{\alpha^2}{2}. \qquad (17)$$

In this expression, θ denotes the beam divergence of the Gaussian laser beam, which is defined as $\theta = 2/(k\omega_0)$. k indicates the laser wavenumber and ω_0 its beam waist. x_0 in (17) denotes the shift or shear between the reference and the test beam, and thus is a parameter for the beam shear. 2α denotes the intersection angle between the test beam and the reference beam. Even when the test beam is perfectly aligned along the verticality, but the test beam intersects the reference beam under this angle, this misalignment produces an error. The gen-

eral case is given by

$$2\alpha = \beta - \gamma, \tag{18}$$

and the respective expression has to be inserted into (17). γ and β describe the angle of the test and the reference beam with respect to the detector plane, respectively. Cavagnero et al.[14] pointed out, that the position and orientation of the detector does not influence the measurement, however the intersection angle between both beams does.

- *Beam verticality*

  If the laser beam is not well aligned along the free fall trajectory of the test mass, the effective wavelength of the laser is changed and thus the result is biased by

  $$\frac{\Delta g}{g} = \frac{\phi^2}{2}, \tag{19}$$

  where ϕ is here the angle of the test beam with respect to the plumb line. This is the cosine error, well known in interferometry. From (17) it can be obtained by setting $\beta = 0$ in (18). $\gamma = 2\alpha$ then represents the intersection angle between both beams. This is equivalent to the case when the angle between the test beam and the plumb line equals $\phi = \gamma/2$, thus we obtain (19). For a gravimeter the alignment along the plumb line has to be done to better than 6×10^{-5} radians, in order to reach the aimed relative uncertainty of 10^{-9}. In our setup this effect is common mode, only the relative parallelism of both beams has to be considered, not the absolute verticality to gravity. Such an angle can easily be verified with the same instrument (a so-called beam checker) as is used for the FG5, for instance. The contribution to the uncertainty is negligible.

  However, a rough alignment with respect to the plumb line has to be done. This is also due to the corner-cube rotation. Corner-cube prisms are in use in this setup. If the laser light is not perpendicular to the base plane of the prism, rotation of the corner-cube during flight can cause a serious bias (see Sec. III C 2).

  It is interesting to note that in principle we can get zero bias, even when the object beam is not well aligned to the verticality. It only matters that the two beams are parallel to each other, when hitting the detector. So, if the verticality is misaligned by δ but the reference mirror is tilted by the same angle, both cosine errors add to zero.

- *Beam diffraction*

  Due to the Gaussian beam profile, the phase of the laser beam is a function of the distance z from the beam waist and of the radial distance from the beam axis. This excess in phase, when compared to an ideal plane wave, gives rise to a different effective wavelength. This in turn results in a bias in the measured g-value. This effect is well known for absolute gravimeters and has been investigated.[15, 16] Van Westrum and Niebauer[15] considered a balanced interferometer, whereas Robertsson[16] gave a more general description including unbalanced inteferometers. Since we have a balanced interferometer, we can use

the simple formula

$$\frac{\Delta g}{g} = \frac{\theta^2}{4} = \frac{\lambda^2}{4\pi^2 \omega_0^2}, \tag{20}$$

for the bias, where λ is the laser wavelength and ω_0 is the beam waist. This is also obtained from (17) by setting $x_0 = 0$ and $\alpha = 0$. After Robertsson, the uncertainty can be estimated with

$$\frac{d(\Delta g)}{d\omega_0} = \frac{-2g}{k^2 \omega_0^3}, \tag{21}$$

where $k = 2\pi/\lambda$ is the wave number and λ is the laser wavelength. For our parameters ($\omega_0 = 3 \times 10^{-3}$ m, $v = 4 \times 10^{-1}$ m s^{-3}, $T = 0.130$ s) and an assumed uncertainty in the beam waist of $u_{\omega_0} = 0.1 \times 10^{-3}$ m, we get $\Delta g_{\omega_0} = 1.2 \times 10^{-7}$ μGal for the bias and 7.6×10^{-9} μGal for its uncertainty.

2. Laser stability

The laser used in the setup is a polarization stabilized Helium-Neon laser (ML-1, from Microg-LaCoste).

Although it would not be necessary to use such a stabilized laser, for the aimed relative uncertainty is of the order of 10^{-4}, we are using the laser in the locked mode. Its specifications show a long term frequency stability of 2×10^{-9}. The contribution to the uncertainty budget is negligibly small.

Non-constant frequency drifts in the laser could also lead to fake accelerations if the path lengths of the two beams were different. Thanks to the equal path length design of the interferometer, this effect, however, is suppressed.

3. Clock stability

For the setup we use an atomic clock with a relative stability of the order of 10^{-10}. The internal clock of the Analog-to-Digital Converter (ADC) has a stability of 1×10^{-5} what would be good enough for our purposes. Experiments, where the external atomic clock was disconnected showed indeed no change in the results. Nevertheless we are using the atomic clock and regard the contribution to the uncertainty budget due to clock stability as negligible.

4. Speed of light

In free fall absolute gravimeters corrections due to the finite propagation velocity of light can reach more than 10 μGal[17] for an acceleration of 9.81×10^8 μGal. Since our expected signal is of 100 μGal and the initial velocities of the test masses are much lower (in a FG5 it is about 0.25 m s^{-1}), the speed of light effect will be of less than 10^{-7} μGal.

5. Vacuum

In order to describe effects which arise from a non-perfect vacuum, we use the ideal gas law and work in the molecular regime (small pressures). Formulas are taken mainly from Ref. 18.

- *Drag effect (Viscosity).* If a plate moves tangentially in a fluid, the plate is subject to a breaking force. This force arises from a momentum transfer of residual gas molecules of the vacuum to the moving plate. For our applications, we model a test mass as a solid cylinder of length $l = 9.375$ cm and a diameter $d = 3.4$ cm. The lateral area is $A_l = d\pi l = 1.00 \times 10^{-2}$ m^2. We assume that the gas particles have no tangential velocity component. The breaking force can then be described by

$$F_R = \frac{2}{\pi} p A_l \sigma_t \frac{v}{\bar{c}} , \qquad (22)$$

where the pressure $p = 1.3 \times 10^{-4}$ Pa, the maximum free-fall velocity is $v = 1.29$ m s^{-1}, the mean gas velocity is $\bar{c} = 463$ m s^{-1}, and the ratio between the mean tangential velocity of the reflected gas particles and the velocity of the moving cylinder is $\sigma_t \approx 1$. For a test body of mass $m_{TM} = 0.150$ kg the deceleration amounts to $a = 1.54\,\mu$Gal. This effect, however, is largely compensated by the use of a co-moving or drag-free chamber.[10] The residual gas particles in the elevator fall with the same velocity as the test mass. Hence, the differential tangential velocity is zero.

Now lets consider the cross-sectional areas. If the test mass is not moving, the gas particles are hitting both areas with the mean gas velocity $\bar{c}$, which results in an equal momentum transfer in both directions. However, if the test mass moves, the mean gas velocity at the lower area becomes $\bar{c} + v$ and at the upper area $\bar{c} - v$. The number of particle hitting the area per unit time can be given as

$$j_{N,l/u} = \frac{p}{4\,kT}(\bar{c} \pm v), \qquad (23)$$

for the lower and upper area. The differential number is then

$$\Delta j_N = \frac{p}{2\,kT}v, \qquad (24)$$

which amounts to $\Delta j_N = 2.07 \times 10^{16}$ s^{-1}m^{-2}, with $k = 1.38 \times 10^{-23}$ J K^{-1} and a temperature of $T = 293$ K. Since the gas molecules enter only through the two holes, which permit to enter the laser light, the cross-sectional area reduces to $A_C = 1$ cm^2. With a free-fall time of $t = 0.131$ s the number of particles becomes $N_c = \Delta j_N t A_c = 2.72 \times 10^{11}$. For the lateral area we get $N_l = 4.88 \times 10^{15}$. We conclude then that the breaking force due to the cross-sectional areas is $\frac{N_c}{N_l} = 5.57 \times 10^{-5}$ times the value due to the lateral area, i.e., amounts to $8.58 \times 10^{-5}\,\mu$Gal.

- *Outgassing.* The ion pump used has a pumping speed of 8 l/s. Taking a mean molar mass of a gas mixture (air) of $\overline{M} = 28.964 \times 10^{-3}$ kg mol^{-1} (see Ref. 18), the density of air in the instrument can be estimated to be $\rho_{vac} = 1.66 \times 10^{-9}$ kg m^{-3}. Here we used the ratio between the pressure within the vacuum chamber of 1.3×10^{-4} Pa and the normal pressure, which is 1.01325×10^5 Pa. It follows that 1 l weighs 1.66×10^{-12} kg. The mass flux thus becomes $Q = 8$

$\times 1.66 \times 10^{-12}$ kg s$^{-1} = 1.33 \times 10^{-11}$ kg s^{-1}. The surface area of the test mass model is $A = 118.3$ cm^2. The dropping chamber can be modeled as a hollow cylinder 80 cm long and with a diameter of 10 cm. Both parts, i.e., the test mass and the dropping chamber, are made from the same material, namely, aluminum. The ratio between both areas becomes $r = 1.88 \times 10^{-2}$. As a result, each test mass looses $\Delta m_{TM} = 1.09 \times 10^{-14}$ kg of weight per second. The momentum transfer is then $\Delta p = \Delta m_{TM}\bar{c} = 5.05 \times 10^{-12}$ kg m s^{-1}. For the deceleration we obtain thus $a = \Delta p/(\Delta t m_{TM}) = 2.57 \times 10^{-2}\,\mu$Gal. Since the middle test mass has a different mass and surface area this can give a systematic offset.

- *Buoyancy.* The buoyant force acting on a test mass equals $a = \frac{\rho_{vac}}{\rho_{TM}}g$. If the test mass is modeled as a cylinder made from aluminum with density $\rho_{TM} = 4.5 \times 10^3$ kg m^{-3} and the density of vacuum is $\rho_{vac} = 1.66 \times 10^{-9}$ kg m^{-3}, then the buoyant force becomes $a = 4 \times 10^{-4}\,\mu$Gal. If the density of all three test masses is equal the differential acceleration becomes negligible.

  For the pressure is a function of height, we can calculate the differential buoyant forces at each test mass due to the barometric formula. This however is by a factor 5×10^5 times smaller than the primary buoyant force.

- *Temperature gradient.* Pressure is also a function of temperature. If there is a temperature gradient along a test mass, the pressure at both ends will differ and thus induce a force onto it. The resultant force becomes $\Delta F = \frac{\Delta T}{T} p A$. With $\Delta T = 0.1$ K denoting the temperature difference at both ends of the test mass, $T = 293$ K, $p = 1.3 \times 10^{-4}$ Pa, and $A = 3.63 \times 10^{-3}$ m^{-2}, the resulting acceleration amounts to $a = 0.11\,\mu$Gal. In our laboratory, we measured a temperature gradient of 1.67 K m^{-1}. Assuming a length of 10 cm for the test mass the acceleration becomes $a = 0.18\,\mu$Gal.

  If all three test masses have the same length and mass, only the machining tolerances need to be considered. These, however, are by a factor 10^{-3} smaller, resulting in $1.8 \times 10^{-4}\,\mu$Gal.

6. Magnetic fields

Magnetic fields can give rise to a huge bias, if wrong materials are used.[11] Niebauer *et al.*[10] derived an estimation for a linear magnetic field of $B_0 = 1$ mT. The test mass was modeled as an aluminum ring falling in this field. For a test mass of $m = 130$ g, they obtained an uncertainty of $a_{B_0} = 10^{-6}\,\mu$Gal. Tests with magnetic fields of the order of 100 μT showed them no detectable bias.

We have not performed any test of this kind so far, but we are planning to do so. We thus attribute an uncertainty of $1 \times 10^{-6}\,\mu$Gal to possible disturbing magnetic fields. We should also bear in mind that we can calibrate the setup before installing the source masses. We only need to be sure that the disturbing fields do not change in time to significant order.

7. Electrostatic forces

The dropping chamber of the gradiometer is made from aluminum and functions as a Faraday cage, shielding the test masses from external electric fields. The only concern is a contact voltage which would arise between the support and the test mass at rest. Niebauer et al.[10] estimated this effect to be of the order of 10^{-5} μGal. This is when a separation of 1 mm is assumed. For our setup is similar to the FG5 and the materials used are similar, we can take this number as a good estimate. Due to the differential measurement this effect will be even further reduced. It must also be noticed that the force arising from the contact voltage is decaying with the separation squared. Hence reducing further its magnitude.

8. Tilt

The consequences of a tilt of the instrument will be twofold. First, the laser will be not aligned along g anymore. This however is a common mode effect, for the tilt angle of the laser beam is the same for the upper gradiometer as for the lower gradiometer. The error is thus null. Second, a tilt of the setup will change the position of the source masses with respect to the test masses. This error will be considered in Subsection III C.

9. Radiation pressure

When the laser light is reflected by the falling body's retroreflector, a momentum is transferred to the falling body, which decelerates it. This momentum equals approximately twice the photon momentum. It is interesting and instructive to treat this problem in a more rigorous way. In order to do so we will use the theory of Compton scattering. In a general case, where the photon hits the mirror with an angle ϕ (it denotes the angle between the photon before and after the scatter), the formula to obtain the energy of the reflected photon is given as

$$E'_f = E_f \frac{1 - \beta \cos \Omega}{(1 - \beta \cos \Omega') + \frac{hf}{\gamma mc^2}(1 - \cos \phi)}, \quad (25)$$

where $\beta \equiv \frac{v}{c}$, $\gamma \equiv \frac{1}{\sqrt{1-\beta^2}}$, v denotes the velocity of the falling object, Ω is the angle between the photon's and falling body's momentum vector before and Ω' after the scatter. h denotes Plancks constant, c the velocity of light, and m the mass of the falling body. If we assume a total reflection with the photon hitting the mirror surface perpendicular (thus, $\Omega = \pi$, $\Omega' = 0$, and $\phi = \pi$), (25) simplifies to

$$E'_f = E_f \frac{1 + \beta}{1 - \beta + \frac{2hf}{\gamma mc^2}}. \quad (26)$$

The frequency shift can then be approximated by

$$\Delta f \approx f \left(1 + 2\frac{v}{c} + 2\frac{v^2}{c^2} - \left(1 + 3\frac{v}{c} + \frac{9}{2}\frac{v^2}{c^2}\right)\frac{2hf}{\gamma mc^2}\right). \quad (27)$$

It can be readily seen that the frequency of the photon is subject to two consecutive Doppler shifts, which is consistent with the theory developed in Ref. 17. The correction term

arises from the Compton effect, which is most easily seen, if we set $v = 0$. Then we get

$$\lambda_C := \lambda' - \lambda = \frac{2h}{mc}, \quad (28)$$

which is the Compton wavelength of the falling body.

The transferred momentum is obtained from momentum conservation. If $\vec{p}$, $\vec{p}'$ denote the momenta of the falling body before and after the scatter, respectively, and $\vec{p}_f$, $\vec{p}'_f$ the momenta of the photon before and after the scatter, respectively, we then have

$$\vec{p}' = \vec{p} + p_f \vec{n} - p'_f \vec{n}'. \quad (29)$$

After multiplication with $\vec{n}'$ we finally get

$$p' = p - 2p_f + \Delta p_f, \quad (30)$$

where $\vec{n}$ and $\vec{n}'$ denote the unit vectors pointing in the direction of the photon before and after the scatter, respectively. This shows that the transferred momentum consists of two terms. The first term is twice the momentum of the photon, which is usually considered for the radiation pressure effect. The term Δp_f can be quantified by the energy change of the photon of Eq. (25), or via the frequency shift formula (27). The term Δp_f consists of two momenta. The first is due to the Doppler shift and becomes

$$p_D = \frac{fh}{c}\left(2\frac{v}{c} + 2\frac{v^2}{c^2}\right). \quad (31)$$

The second is due to the Compton scatter, which is

$$p_C = -f\left(1 + 3\frac{v}{c} + \frac{9}{2}\frac{v^2}{c^2}\right)\frac{2hf}{mc^2}. \quad (32)$$

Assuming a mass of the falling body of $m = 0.130$ kg and a free fall time of $t = 0.2$ s, the deceleration of the falling body due to the photon reflection is

$$a_f = \frac{2P_l}{mc} \approx 5.1 \times 10^{-3} \ \mu\text{Gal}, \quad (33)$$

for a 1 mW HeNe laser. The correction due to the Doppler term is eight orders of magnitude, and the Compton term 35 orders of magnitude smaller, respectively.

It is interesting to note that the Compton term leads to the wrong conclusion that objects of different masses are subject to different accelerations, contrary to the equivalence principle. This would be noticeable only at the order of 10^{-35} for our setup. In case of atoms or electrons, however, the effect would be far bigger and should be taken into account.

10. Self-attraction due to instrument

The gradiometer has a proper mass which generates a gravity field. This field is in general neither homogeneous nor linear and thus has a different value at every position of the test masses. The result would be a measured differential acceleration which gives a bias when measuring G. To minimize this problem, we could perform a measurement without any source mass and thus adjust the gradiometer. The other possibility is to calculate the proper field from the technical drawing. This is done with classical free fall absolute

gravimeters[19–21] as well as with cold atom gravimeters.[22] The parts of the gravimeters are then either roughly estimated by measuring them and building a simple model[19–21] (e.g., rods, tubes, blocks) or from the technical drawing using the finite element method.[22] So far we did not evaluate the self-attraction for our setup. We plan to build a finite element model. This modeled acceleration will be integrated twice in time, in order to get the distance bias as function of time. A correction is straightforward by applying a least squares adjustment with our model function for the free fall trajectory. If in addition, we adjust the setup by performing measurements without source masses, a standard uncertainty of less than a nanogal should be feasible.

11. Environmental effects

- *Pressure*. For free-fall absolute gravimeters a correction is applied for an environmental pressure that differs from the defined nominal pressure

$$P_n = 1013.25 \times \left(1 - 0.0065 \, \frac{h_m}{288.15} \right). \qquad (34)$$

The change in gravity comes because high pressure is due to higher density of the atmosphere. This higher density results in a higher attraction of the test mass upwards, i.e., the measured gravity is lower. The barometric factor is defined as $f_B = 0.3 \, \mu$Gal hPa^{-1}.
For the differential measurement this effect is completely canceled out and can be omitted, since the atmospheric attraction can be taken as homogeneous and is thus equal for all three test mass positions.

- *Tides and Ocean loading*. Tidal variations as well as ocean loading effects are the same for all three test masses. By means of the differential nature of the instruments, those effects are null.

C. Non-differential mode uncertainties

1. Test mass positioning errors

- *Initial velocity*. In order to apply the zerocrossing method to determine the acceleration, we need to have fringes. However, the expected signal of 100 μGal produces an optical path change of only 8.6 nm, too small to produce a single fringe. It is difficult to get the phase change out of an almost DC signal. A way to still be able to apply the familiar zerocrossing detection is to generate a background frequency onto which the acceleration is frequency modulated. This could be done by means of an acousto-optical modulator (AOM), which shifts the frequency in one arm of the interferometer. In our setup we use another solution. A custom made support ring (see Figure 4), which supports the middle test mass, acts like a trampoline. When the elevator is accelerated the middle test mass is then released at a later time, so that it starts with another initial velocity. This initial velocity produces a basic signal of approximately 12 kHz, which can be used then for a zerocrossing detection. Since the
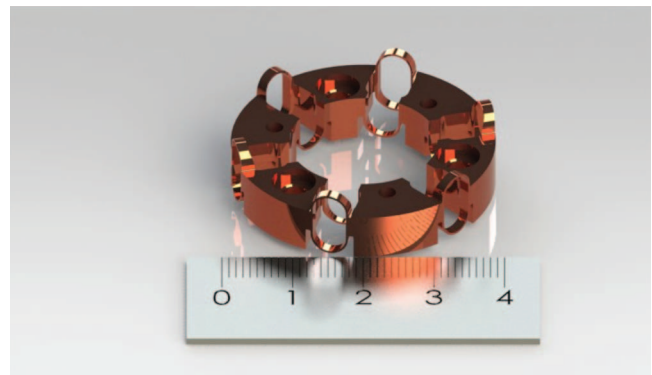

FIG. 4. Trampoline-like plate that gives an initial velocity to the middle test mass (units on scale are in centimeters). This creates a basic frequency of approximately 12 kHz. (Courtesy: Micro-g LaCoste.)

middle test mass is dragged with respect to the other two ones, we have to take into account the new position with respect to the source masses. However, it can be shown that this initial velocity is of the order of 4×10^{-3} m s^{-1}. The resulting dragged distance thus amounts to about 7.5×10^{-7} m, i.e., less than 1 μm. Given a local gravity gradient of $\gamma = 300 \, \mu$Gal m^{-1}, this results in an uncertainty of $10^{-4} \, \mu$Gal.

2. Corner cube rotation

The instrument contains four prism corner cube reflectors, which are mounted in three test bodies. The middle test body contains two reflectors, whereas the upper and the lower test body contain only one. From free fall gravimeters it is well known that a rotation of the test body during free fall can give rise to a bias in the acceleration due to gravity. This is due to the rotation of the optical center of the retroreflector about the center of mass of the whole test body, if those two points do not coincide; rotation itself is unavoidable unfortunately, though it can be minimized. In Ref. 23, this effect and an additional one, which arises from the refractive index of the prism, are described. For an uncertainty estimation we assume that the plain surface of the prism is tilted by less than 1° with respect to the horizontal and that the rotational velocity of the test body is less than 10 mrad s^{-1}. The center of mass of the test body can be shifted to the optical center to better than 25 μm. With a drop time of 0.131 s the uncertainty due to the refractive index amounts to $8.7 \times 10^{-4} \, \mu$Gal, whereas for the finite distance between the two centers we obtain $4.6 \times 10^{-3} \, \mu$Gal. This results in a combined standard uncertainty of $8.1 \times 10^{-3} \, \mu$Gal for all three test masses.

It should be noted that for the middle test mass the center of mass cannot be shifted to the optical centers of both retroreflectors at the same time. However, if the position of the center of mass lies exactly at half the distance between both optical centers, the effect cancels out, since it becomes common for the upper and the lower optical path.

3. Source mass density inhomogeneities and positioning errors

So far the source masses are still in a planning stage. We cannot give a precise uncertainty, however from other

experiments we can estimate what is at least doable. In a cold atom gravimeter version of the G-measurement the relative standard uncertainty – mainly from positioning errors – was of about 4.6×10^{-4} [9] for a total source mass of about 500 kg of tungsten. Schwarz *et al.* reported a relative standard uncertainty of 160×10^{-6} due to positioning errors and source mass density variations.[7] In a beam balance experiment at the University of Zurich two cylindrical vessels, filled with 14 metric tons of mercury were used.[3] Their result is the second best measurement ever made, with a relative standard uncertainty of 21×10^{-6}. Although mercury has a good density homogeneity and high density, it is a delicate material due to its toxicity.

Our plan is to use numerous small metal spheres instead of big cylinders as done by Schwarz *et al.*[7] or Lamporesi *et al.*[9] Let us make some basic considerations in order to compare solid cylinder source masses with approximately the some volume filled with spheres. Assume 12 identical solid cylinders with a height of $h = 15$ cm and radius of 5 cm. Arrange them in order to give a hexagonal ring shape with an inner diameter of 10 cm. The outer diameter then becomes 44 cm, like in Lamporesi *et al.*[9] If we fill this volume with spheres (close packing), then the occupied volume by the material is in the case of the cylinders 8.8% bigger than with spheres (With close packing the occupied space is 74% of the total volume). However, spheres are cheaper and give a more homogeneous density distribution.

Let us compare the uncertainties. Assume a relative uncertainty in the density of the cylinders of 6.6×10^{-4}. The relative uncertainty in G becomes then from 12 cylinders 2×10^{-4}. A sphere, on the other hand, can be manufactured to a tolerance of $\Delta d = 5.32 \times 10^{-6}$ m (grade G3). We can assume that the homogeneity through a sphere is almost perfect. The uncertainty arises then only from the shape, i.e., the volume. The relative uncertainty in G can then be expressed as $1/\sqrt{n-1} \times 3 \times \Delta R/R$, where n denotes the number of spheres, R the nominal radius of the spheres, and ΔR the production tolerance of the spheres. Table II shows the relative uncertainties in G, as a function of R. It turns out that a relative uncertainty below 1×10^{-5} can be reached if spheres of a diameter of 5 mm with tolerance of grade G3 are used.

4. Beam shear

In Sec. III B 1, we treated already beam verticality and diffraction effects. The formula (17), however, includes also the case when the test and reference beam are not coaxial, but are subject to a lateral shift x_0. α in Eq. (17) is assumed to be zero. It can be seen that a lateral shift reduces the bias due to

TABLE II. Uncertainty due to manufacturing tolerances of spheres. n – number of spheres; ΔR – tolerance of radius; R – Radius of sphere.

R (mm)	2.5	5	10
ΔR (mm)	3×10^{-3}	3×10^{-3}	5×10^{-3}
n	198 540	24 817	4192
$\Delta G/G$	8×10^{-6}	1.2×10^{-5}	4.7×10^{-5}

diffraction. Since the beams are aligned in a way as to be as coaxial as possible, we can neglect this effect.

5. Coriolis effect

All three test masses are sitting on vee-groves in their drag-free chamber. The three drag-free chambers, on the other hand, are connected to the same elevator. At the beginning of the drop, the elevator is accelerated towards the earth faster than the acceleration due to gravity, g. In an ideal case the test masses will just hover from the vee-groves and fall freely along the plumb line. Due to coupling forces between the test masses and the support ring, which contains the vee-groves, the test masses can be dragged along with the elevator for a short time. If the elevator, in addition, is not well aligned along the plumb line, the dragging vector will contain a horizontal component. As a consequence, the test mass will acquire a horizontal velocity component, and together with earth's rotation this gives rise to a Coriolis force acting on it, and thus result in a bias of g. The Coriolis acceleration can be described by

$$a_{Cor} = 2\Omega_N v_{EW} \sin\left(\frac{\pi}{2} - \theta\right), \qquad (35)$$

where v_{EW} denotes the velocity in the east-west direction. $\Omega_N = 7.2921151467064 \times 10^{-5}$ rad s^{-1} is the nominal angular velocity of the earth and $\theta \approx 50°$ is the latitude of the site of measurement (Luxembourg). In order to estimate v_{EW}, we move the elevator up and down and observe the reflected laser spot, which moves horizontally, if the rail, on which the elevator moves, is not well aligned along the plumb line. The range the elevator can be moved is about 100 mm. If we assume a maximum horizontal movement of the spot by 0.5 mm in a distance of 1 m, the horizontal displacement of the test mass over the range of 100 mm will be 0.05 mm. This gives an angle of 5×10^{-4} rad with respect to the plumb line. The acceleration of the elevator at the start of the drop is about 11 m s^{-2}. Let us estimate the drag time with 10 ms. Then we get for the horizontal velocity $v_{EW} = 1.1 \times 10^{-5}$ m s^{-1}. With the latitude for Luxembourg, the acceleration amounts to 0.1 μGal. This, however, is a worst case effect. It can be greatly reduced by aligning the carriage so that the horizontal velocity points into the north-south direction, as described by Niebauer *et al.*[10] Furthermore, all three test masses are sitting in the same carriage, so that their horizontal velocities will be approximately the same. We believe that an uncertainty of 0.01 μGal is more realistic.

6. Two-sample zerocrossing

The differential acceleration of the three test masses is obtained by analysing the fringe signal for the relative time occurrences of zerocrossings, which provides us the information about time and position of the test masses. This is a well-established method, which is also employed in common free-fall gravimeters. By determining the zerocrossing, we have to look into the signal and find two consecutive amplitude values were the sign changes. In order to determine this timing occurrence more precisely a linear interpolation is applied to

those two points. In order to quantify the remaining uncertainty due to this interpolation onto the acceleration, we use the approach found in[24]

$$\sigma_g \approx \eta \frac{6\sqrt{2}}{T^2} \frac{\lambda}{\sqrt{N}} \times \sigma_\phi \, , \qquad (36)$$

where λ is the wavelength of the laser, T is the total drop time, N is the number of zerocrossings, which can be calculated from the signal frequency f_0 and the drop time T. η is an instrument-specific parameter, which depends on the initial velocity, the acceleration and the drop time (see Ref. [25]). For our parameters $\eta \approx 1$. Besides the uncertainty due to interpolation σ_ϕ can contain also an uncertainty due to digitization. After[24] the interpolation uncertainty can be quantified as

$$\sigma_{\phi,int} = 0.45 \times \left(\frac{f_0}{f_S} \right)^3 \, , \qquad (37)$$

and the error due to digitization as

$$\sigma_{\phi,quant} = \frac{1}{4\pi} \frac{1}{10^{\frac{SNR}{20}}} \, . \qquad (38)$$

The SNR can be obtained from the specifications of the digitizing card in use. f_0 denotes the signal frequency and f_S the sampling rate of the digitizer. As an example, if we have $f_0 = 12$ kHz, $f_S = 100$ kHz, and $SNR = 69$ dB (SINAD of our ADC GAGE Applied, model CompuScope CS144002U), then the quantization uncertainty amounts to $\sigma_{g,quant} = 1.18 \times 10^{-2} \mu$Gal, and the interpolation uncertainty $\sigma_{g,int} = 4.34 \times 10^{-1} \mu$Gal, i.e., a combined standard uncertainty of $\sigma_g = 4.34 \times 10^{-1} \mu$Gal. This type A uncertainty can be largely reduced by a repetition of the measurement. With 100 measurements this uncertainty will be reduced by a factor of 10. For the expected signal of 100 μGal this would give a relative uncertainty of 4.34×10^{-4}. The accuracy assessment, presented in Ref. [24], provides us the possibility to find the optimum parameters to reach the desired relative uncertainty in G. For instance, if we are able to increase the basic frequency f_0 to 1 MHz and sample with $f_S = 100$ MHz, then we would get $\sigma_{g,quant} = 1.72 \times 10^{-3} \mu$Gal for the quantization uncertainty and $\sigma_{g,int} = 2.75 \times 10^{-5} \mu$Gal for the interpolation uncertainty, which satisfies our requirements.

Unfortunately, we are not able to tune the support ring of the middle test mass in order to increase the initial velocity. This is why we have to go another way to get the desired 1 MHz. A possibility would be to mix the analog fringe signal with a very stable 1 MHz signal. The resultant beat signal would then be of approximately 1 MHz.

D. Combined uncertainty budget

In the following Table III, we list all error sources considered so far. The relative uncertainty is given for a hypothetical source mass producing a signal of 100 μGal.

IV. DISCUSSION AND CONCLUSION

Our feasibility study showed that with our current setup a measurement of G could be done with a relative standard uncertainty of smaller than 5.3 parts in 10^4. This would not

TABLE III. Table of all considered sources of uncertainty given as relative standard uncertainty; signal of 100 μGal is assumed.

Error source	Relative uncertainty
Beam verticality	1×10^{-9}
Beam diffraction	1.2×10^{-9}
Laser stability	2×10^{-9}
Clock stability	1×10^{-10}
Speed of light	1×10^{-9}
Drag effect	1×10^{-6}
Outgassing	2.6×10^{-4}
Buoyancy	negligible
Temperature gradient	1.8×10^{-6}
Magnetic fields	1×10^{-6}
Electrostatic forces	1×10^{-7}
Radiation pressure	5.1×10^{-5}
Self attraction	1×10^{-5}
Environmental effects	negligible
Initial velocity of test mass	3×10^{-6}
Corner cube rotation	8.1×10^{-5}
Source mass (density/positioning)	1×10^{-5}
Beam shear	negligible
Coriolis effect	1×10^{-4}
Two-sample zerocrossing	4.4×10^{-4}
Combined standard uncertainty	5.3×10^{-4}

be better than the uncertainty in the current CODATA value. However, with some improvements our aim could be reached. A first step could be done by replacing our trampoline-like support of the middle test mass by an Acousto optic modulator, in order to increase the base frequency of our signal and thus lower the uncertainty due to zerocrossing detection. It has been shown that an uncertainty of $2 \times 10^{-3} \mu$Gal is reachable for a base frequency of 1 MHz and a sampling rate of 100 MHz, with our current DAC card. The uncertainty due to outgassing is another issue in our current setup. This could be reduced by improving the vacuum, using a bigger ion pump. The third problem is Coriolis force. So far its magnitude seems to be overestimated. Further tests must be done to quantify this effect and possibly better alignment will reduce it greatly.

In conclusion, we have presented a novel setup to measure small local gravity inhomogeneities. The principle of measurement is similar to classical free fall absolute gravimeters, like the well-known FG5, from Micro-g LaCoste Inc. The difference to those gravimeters is that the differential acceleration of three simultaneously falling objects is measured, thus measuring the second vertical derivative of the acceleration due to gravity, g. The instrument can be considered as a null instrument, for if the gravity is constant or linearly changing with height (constant gradient) the measured signal is zero. This highly sensitive instrument will be used to measure the Gravitational Constant, G, in a future experiment, with an uncertainty probably better than 1 part in 10^4.

ACKNOWLEDGMENTS

APPENDIX: HOW TO FIND THE OPTIMUM POSITION OF THE TEST MASSES

Unfortunately, the gravity field is not constant over the whole drop range of the test masses. The measured gravity signal will rather be a weighted mean value over the nonlinear gravity field. It is important therefore to determine the position where, first, the error due to imperfect positioning is least and, second, the signal is maximized.

Nagornyi[26] suggested a method to calculate the correction for small (in comparison to Earth's gravity) disturbing fields in the case of free-fall gravimeters. He proposes that the measured (correction) value of gravity should be found as a mean-weighted value of the acceleration of a freely falling body averaged within every measurement. The correction in the true value can thus be found as

$$\overline{\Delta g} = \int_a^b \Delta g(t)\omega(t)dt, \tag{A1}$$

where Δg is the perturbing field, the correction of which wants to be determined, $\omega(t)$ is the weighting function, and a, b are the limits of integration, which are usually taken as $a = 0$ and $b = T$ (T being the total free-fall time) for free-fall gravimeters. The weighting function depends on the model function that is fitted to the measured trajectory. For the second order model function

$$z(t) = z_0 + v_0 t + \frac{g}{2}t^2, \tag{A2}$$

where z_0 denotes the initial position, v_0 some initial velocity, and g the acceleration due to gravity, the weighting function can be found by means of

$$\omega(t) = \frac{1}{P}\sum_{i=1}^{5} K_i t^i, \tag{A3}$$

for the SD case (data are equally spaced in distance), with (see Ref. [26]),

$$
\begin{aligned}
K_1 &= 0 \\
K_2 &= \frac{v_0^3 T^2}{18} + \frac{v_0^2 g T^3}{15} + \frac{v_0 g^2 T^4}{60} \\
K_3 &= -\frac{v_0^3 T}{9} - \frac{v_0^2 g T^3}{10} + \frac{g^3 T^4}{180} \\
K_4 &= \frac{v_0^3}{18} - \frac{v_0 g^2 T^2}{20} - \frac{g^3 T^3}{90} \\
K_5 &= \frac{v_0^2 g}{30} + \frac{v_0 g^2 T}{30} + \frac{g^3 T^2}{180} \\
P &= \frac{v_0^3 T^5}{540} + \frac{v_0^2 g T^6}{360} + \frac{v_0 g T^7}{900} + \frac{g^3 T^8}{10800}.
\end{aligned}
\tag{A4}
$$

For negligible velocities this expression reduces to

$$\omega(t) = 60\frac{t^3}{T^4} - 120\frac{t^4}{T^5} + 60\frac{t^5}{T^6}. \tag{A5}$$

Once the weighting function is determined the correction to a perturbing gravity can be calculated. To do so the perturbing gravity has to be given as a polynomial.

1. Examples

As a first example let us consider the field which has a constant gravity gradient γ,

$$\Delta g = z(t)\gamma . \tag{A6}$$

The correction is then found by means of (A1),

$$\overline{\Delta g} = \gamma \int_0^T z(t)\omega(t)dt. \tag{A7}$$

Inserting Eqs. (A2) and (A5) yields

$$\overline{\Delta g} = \gamma \int_0^T \left(\frac{1}{2}gt^2 + v_0 t + z_0\right) \\ \times \left(60\frac{t^5}{T^6} - 120\frac{t^4}{T^5} + 60\frac{t^3}{T^4}\right) dt. \tag{A8}$$

This expression has to be integrated to give the gravity correction. It is, however, more instructive to write

$$
\begin{aligned}
\overline{\Delta g} &= \gamma \int_0^T \left(\frac{1}{2}gt^2 + v_0 t + z_0\right)\omega(t)dt \\
&= a_2 \int_0^T \omega(t)t^2 + a_1 \int_0^T \omega(t)t + a_0 \int_0^T \omega(t),
\end{aligned}
\tag{A9}
$$

where we set

$$a_2 := \gamma \frac{1}{2}g \qquad a_1 := \gamma v_0 \qquad a_0 := \gamma z_0. \tag{A10}$$

The factors

$$c_n := \int_0^T \omega(t)t^n dt \tag{A11}$$

are called the *moments*. So we can write instead of (A9)

$$\overline{\Delta g} = a_2 c_2 + a_1 c_1 + a_0 c_0, \tag{A12}$$

or more general

$$\overline{\Delta g} = \sum_{n=0}^{N} a_n c_n, \tag{A13}$$

where N is the maximum order to which t appears. The moments are functions of the model function only, for instance, for

$$
\begin{aligned}
c_3 &= \int_0^T \omega(t)t^3 dt = \int_0^T \left(60\frac{t^5}{T^6} - 120\frac{t^4}{T^5} + 60\frac{t^3}{T^4}\right)t^3 dt \\
&= T^3 \frac{5}{21}.
\end{aligned}
\tag{A14}
$$

A calculation with MAPLE gives the following moments for negligible initial velocities:

$$
\begin{array}{ccc}
c_0 = 1 & c_1 = \frac{4}{7}T & c_2 = \frac{5}{14}T^2 \\[2mm]
c_3 = \frac{5}{21}T^3 & c_4 = \frac{1}{6}T^4 & c_5 = \frac{4}{33}T^5 \\[2mm]
c_6 = \frac{1}{11}T^6 & c_7 = \frac{10}{143}T^7 & c_8 = \frac{5}{91}T^8 \\[2mm]
c_9 = \frac{4}{91}T^9 & c_{10} = \frac{1}{28}T^{10} & c_{11} = \frac{1}{34}T^{11} .
\end{array}
\tag{A15}
$$

For non-negligible velocities the moments become more complex:

$$c_0 = 1$$

$$c_1 = \frac{1}{7}\frac{T\left(108v_0^2 gT + 45v_0 g^2 T^2 + 4g^3 T^3 + 70v_0^3\right)}{20v_0^3 + 30v_0^2 gT + 12v_0 g^2 T^2 + g^3 T^3}$$

$$c_2 = \frac{1}{14}\frac{T^2\left(126v_0^2 gT + 54v_0 g^2 T^2 + 5g^3 T^3 + 80v_0^3\right)}{20v_0^3 + 30v_0^2 gT + 12v_0 g^2 T^2 + g^3 T^3}$$

$$c_3 = \frac{5}{42}\frac{T^3\left(48v_0^2 gT + 21v_0 g^2 T^2 + 2g^3 T^3 + 30v_0^3\right)}{20v_0^3 + 30v_0^2 gT + 12v_0 g^2 T^2 + g^3 T^3}$$

$$c_4 = \frac{1}{42}\frac{T^4\left(162v_0^2 gT + 72v_0 g^2 T^2 + 7g^3 T^3 + 100v_0^3\right)}{20v_0^3 + 30v_0^2 gT + 12v_0 g^2 T^2 + g^3 T^3}$$

$$c_5 = \frac{1}{66}\frac{T^5\left(180v_0^2 gT + 81v_0 g^2 T^2 + 8g^3 T^3 + 110v_0^3\right)}{20v_0^3 + 30v_0^2 gT + 12v_0 g^2 T^2 + g^3 T^3}$$

$$c_6 = \frac{1}{33}\frac{T^6\left(66v_0^2 gT + 30v_0 g^2 T^2 + 3g^3 T^3 + 40v_0^3\right)}{20v_0^3 + 30v_0^2 gT + 12v_0 g^2 T^2 + g^3 T^3}$$

$$c_7 = \frac{1}{143}\frac{T^7\left(216v_0^2 gT + 99v_0 g^2 T^2 + 10g^3 T^3 + 130v_0^3\right)}{20v_0^3 + 30v_0^2 gT + 12v_0 g^2 T^2 + g^3 T^3}$$

$$c_8 = \frac{5}{1001}\frac{T^8\left(234v_0^2 gT + 108v_0 g^2 T^2 + 11g^3 T^3 + 140v_0^3\right)}{20v_0^3 + 30v_0^2 gT + 12v_0 g^2 T^2 + g^3 T^3}$$

$$c_9 = \frac{1}{91}\frac{T^9\left(84v_0^2 gT + 39v_0 g^2 T^2 + 4g^3 T^3 + 50v_0^3\right)}{20v_0^3 + 30v_0^2 gT + 12v_0 g^2 T^2 + g^3 T^3}$$

$$c_{10} = \frac{1}{364}\frac{T^{10}\left(270v_0^2 gT + 126v_0 g^2 T^2 + 13g^3 T^3 + 160v_0^3\right)}{20v_0^3 + 30v_0 2gT + 12v_0 g^2 T^2 + g^3 T^3}$$

$$c_{11} = \frac{1}{476}\frac{T^{11}\left(288v_0^2 gT + 135v_0 g^2 T^2 + 14g^3 T^3 + 170v_0^3\right)}{20v_0^3 + 30v_0^2 gT + 12v_0 g^2 T^2 + g^3 T^3}.$$

(A16)

Hence, our gradient correction becomes

$$\overline{\Delta g} = a_2 \frac{1}{14}\frac{T^2\left(126v_0^2 gT + 54v_0 g^2 T^2 + 5g^3 T^3 + 80v_0^3\right)}{20v_0^3 + 30v_0^2 gT + 12v_0 g^2 T^2 + g^3 T^3}T^2$$
$$+ a_1 \frac{1}{7}\frac{T\left(108v_0^2 gT + 45v_0 g^2 T^2 + 4g^3 T^3 + 70v_0^3\right)}{20v_0^3 + 30v_0^2 gT + 12v_0 g^2 T^2 + g^3 T^3}T + a_0,$$

(A17)

and with (A10),

$$\overline{\Delta g} = \gamma \frac{1}{2}g\frac{1}{14}\frac{T^2\left(126v_0^2 gT + 54v_0 g^2 T^2 + 5g^3 T^3 + 80v_0^3\right)}{20v_0^3 + 30v_0^2 gT + 12v_0 g^2 T^2 + g^3 T^3}T^2$$
$$+ \gamma v_0 \frac{1}{7}\frac{T\left(108v_0^2 gT + 45v_0 g^2 T^2 + 4g^3 T^3 + 70v_0^3\right)}{20v_0^3 + 30v_0^2 gT + 12v_0 g^2 T^2 + g^3 T^3}T$$
$$+ \gamma z_0,$$

(A18)

or for negligible initial velocities

$$\overline{\Delta g} = \gamma \frac{1}{2}g\frac{5}{14}T^2 + \gamma v_0 \frac{4}{7}T + \gamma z_0. \qquad (A19)$$

This is the correction if a free-fall measurement is conducted where a constant gradient is present. The gradient function (A6) is a first order polynomial in $z(t)$ (In what follows we write z rather than $z(t)$ for the sake of simplicity). In order to extent the method to functions of higher orders in z, we assume a fifth order polynomial

$$\Delta g = b_5 z^5 + b_4 z^4 + b_3 z^3 + b_2 z^2 + b_1 z^1 + b_0 z^0. \quad (A20)$$

The correction we find for this perturbing function is

$$\overline{\Delta g} = \int_0^T \left(b_5 z^5 + b_4 z^4 + b_3 z^3 + b_2 z^2 + b_1 z + b_0\right)\omega(t)dt. \tag{A21}$$

In the next step, we replace z by (A2). For simplicity, we set $v_0 = z_0 = 0$. Then we get

$$\overline{\Delta g} = \int_0^T \left[b_5\left(\frac{g}{2}t^2\right)^5 + b_4\left(\frac{g}{2}t^2\right)^4 + b_3\left(\frac{g}{2}t^2\right)^3 \right.$$
$$\left. + b_2\left(\frac{g}{2}t^2\right)^2 + b_1\left(\frac{g}{2}t^2\right) + b_0\right]\omega(t)dt$$
$$= \int_0^T \left[b_5\left(\frac{g}{2}\right)^5 \omega t^{10} + b_4\left(\frac{g}{2}\right)^4 \omega t^8 + b_3\left(\frac{g}{2}\right)^3 \omega t^6 \right.$$
$$\left. + b_2\left(\frac{g}{2}\right)^2 \omega t^4 + b_1\left(\frac{g}{2}\right)\omega t^2 + b_0\omega\right]dt \qquad (A22)$$

or

$$\overline{\Delta g} = c_{10}\tilde{b}_5 + c_8\tilde{b}_4 + c_6\tilde{b}_3 + c_4\tilde{b}_2 + c_2\tilde{b}_1 + c_0\tilde{b}_0, \quad (A23)$$

where c_n are the moments given by (A15) and

$$\tilde{b}_n = b_n\left(\frac{g}{2}\right)^n. \tag{A24}$$

We see that we are able to obtain the correction for an arbitrary perturbation Δg, without further integration, as long as the perturbation is given as a polynomial. For the correction we then only need to know the model function.

As a second example, we consider a second-order gravity model

$$g = g_M - (z - z_M)^2 \tilde{\gamma}$$
$$= -\tilde{\gamma}z^2 + 2z_M\tilde{\gamma}z + (g_M - z_M^2\tilde{\gamma})$$
$$= p_1 z^2 + p_2 z + p_3, \tag{A25}$$

where we set $p_1 := -\tilde{\gamma}$, $p_2 := 2z_M\tilde{\gamma}$, and $p_3 := (g_M - z_M^2\tilde{\gamma})$. g_M denotes the maximum gravity, s_M is the position of g_M and $\tilde{\gamma}$ is a gradient-like parameter. By inserting (A2) we get

$$g = -\tilde{\gamma}\left(z_0 + v_0 t + \frac{g}{2}t^2\right)^2 + 2z_M\tilde{\gamma}\left(z_0 + v_0 t + \frac{g}{2}t^2\right)$$
$$+ \left(g_M - z_M^2\tilde{\gamma}\right)$$
$$= -\frac{1}{4}\tilde{\gamma}g^2 t^4 - \tilde{\gamma}g v_0 t^3 + \left(z_M\tilde{\gamma}g - gz_0\tilde{\gamma} - \tilde{\gamma}v_0^2\right)t^2$$
$$+ \left(2z_M\tilde{\gamma}v_0 - 2v_0 z_0\tilde{\gamma}\right)t + \left[2z_M\tilde{\gamma}z_0 - \tilde{\gamma}z_0 - \tilde{\gamma}z_0^2\right.$$
$$\left. + \left(g_M - z_M^2\tilde{\gamma}\right)\right]. \tag{A26}$$

Then, for the correction, we get

$$\overline{\Delta g} = -\frac{g^2}{4}\tilde{\gamma}c_4 - \tilde{\gamma}gv_0 c_3 + \left[\tilde{\gamma}g\left(z_M - z_0\right) - \tilde{\gamma}v_0^2\right]c_2$$
$$+ 2\tilde{\gamma}v_0\left(z_M - z_0\right)c_1$$
$$+ \left[2z_M\tilde{\gamma}z_0 + g_M - \tilde{\gamma}\left(z_0^2 + z_M^2\right)\right] \quad \text{(A27)}$$

or, if we assume that $v_0 = z_0 = 0$, then (A27) simplifies to

$$\overline{\Delta g} = -\left(\frac{g}{2}\right)^2 \tilde{\gamma}c_4 + \tilde{\gamma}gz_M c_2 + (g_M - \tilde{\gamma}z_M^2)c_0$$
$$= +\left(\frac{g}{2}\right)^2 p_1 c_4 + \frac{g}{2}p_2 c_2 + p_3 c_0. \quad \text{(A28)}$$

If (A25) describes the field generated by a source mass, then the test mass (falling body) falls only through a short part of it. Depending on which part of the field is taken, the final correction will differ. We can find the start position of the trajectory, for which the correction becomes maximum. Deriving (A28) with respect to z_M gives

$$\frac{d\overline{\Delta g}}{dz_M} = \tilde{\gamma}gc_2 - 2\tilde{\gamma}z_M c_0 = \tilde{\gamma}g\frac{5}{14}T^2 - 2\tilde{\gamma}z_M. \quad \text{(A29)}$$

By Eq. (A29) to zero and solving for z_M we get the position for which the correction results maximum. In other words: Assume that we have a gravity field as depicted in Figure 5. The bold (red) line is the drop range of the test mass. Then, we need to know where we start our drop, when the parameters initial velocity and drop length are fixed. By means of (A29) we find that position to be

$$z_M = g\frac{5}{28}T^2, \quad \text{(A30)}$$

which gives $z_M = 1.75$ cm for $T = 0.1$ s and $g = 9.81$ m s^{-2}. Consequently, we have to start the drop 1.75 cm before the maximum of the gravity field to get a maximum correction.

2. Application

In order to get the best position of the test masses with respect to the source masses, the procedure to determine the correction could look as follows:

1. We simulate the gravity field of the source (and test) mass as function of the position. (In general, this function has a very complex structure for which we hardly can find an analytical form. Hence, we give the perturbing function in equally spaced position intervals to the required resolution for the length of the drop.)

2. We fit a polynomial of nth order to the simulated data. MATLAB uses the function *polyfit* to get the least squares fit for a polynomial function. In the case of

$$p = polyfit(x, y, n) \quad \text{(A31)}$$

the coefficients are returned as a $(n + 1)$-dimensional vector giving the coefficients in descending order:

$$p = (p_n, \ldots, p_1, p_0) \quad \text{(A32)}$$

for the data (x, y). n denotes the requested order of the polynomial. The fitted function is then

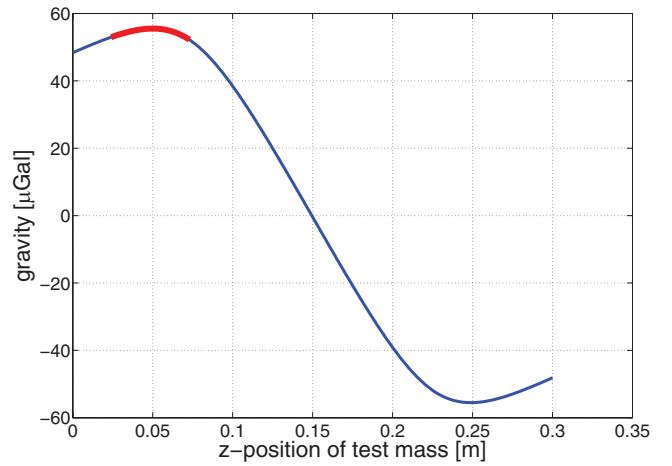$$y = p_n x^n + \ldots + p_1 x + p_0. \quad \text{(A33)}$$

FIG. 5. Gravity field simulation of a torus. The bold (red) part describes the part where the test mass falls through.

Here (A33) has the same form as (A20). This is why we can proceed as we did before. We replace for negligible initial velocities x^n by $c_{2n}(\frac{g}{2})^n$. Then the correction results in

$$\overline{\Delta g} = c_{2n}\left(\frac{g}{2}\right)^n p_n + \ldots + c_2\left(\frac{g}{2}\right)p_1 + c_0 p_0. \quad \text{(A34)}$$

The parameter T in the moments is the total free-fall time. For arbitrary initial velocities and initial positions, the expression for the correction becomes more complex.

A MATLAB program was written in order to determine the correction due to the torus, as simulated in Figure 5. To this end only the part of the gravity field is considered, where the free-fall happens; its gravity is maximum there. A polynomial of, say, fifth order is fitted to this short range of the simulated data that include the maximum; it is indicated in the figure as a bold (red) line and is of 5 cm in our case. The corrected gravity is then obtained by applying Nagornyi's method to the function parameters which were
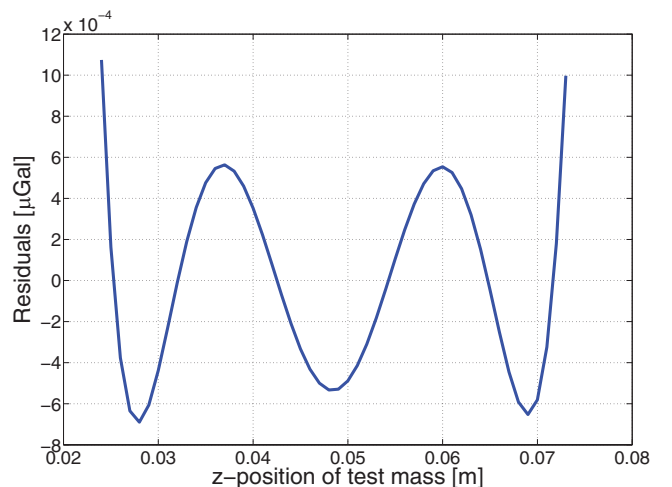

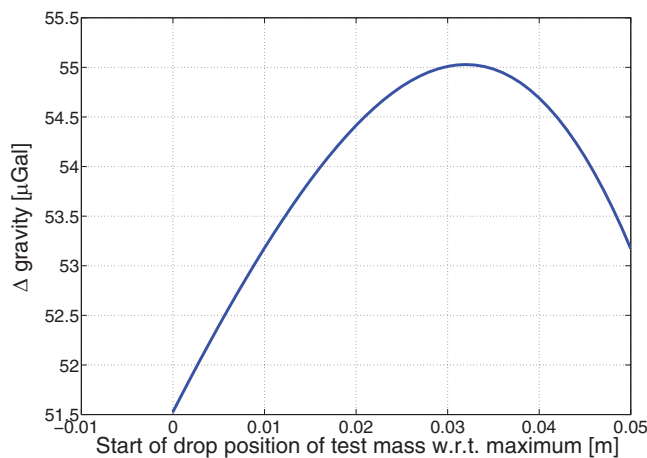FIG. 6. Residuals between the simulated data and the least squares fitted data.

FIG. 7. The gravity correction depends on the initial position of the test mass. Each point of the graph gives the correction for the whole trajectory as function of the start position.

found by means of the fit. Finally, the correction is calculated for different initial positions of the measurement range that always includes the maximum gravity value. With this method we can find the initial position that results in the maximum gravity correction.

Figure 5 shows the simulated gravity of the torus along the axis of symmetry. The drop range is indicated with a bold (red) line. To this bold part a least squares fitting (LSF) to fifth order is applied. The residuals are shown in Figure 6. The values agree in this case to one part in 10^3. With the parameters obtained by the LSF the gravity correction can then be calculated by the method described above. If we maintain the drop range constant, as well as the initial velocity and the acceleration due to gravity, and only change the initial position of the drop range, we can get knowledge about how the corrected gravity depends on the initial position. This issue is depicted in Figure 7. We can see that the correction reaches a maximum, when the drop starts at about 1.8 cm before the maximum. This result agrees very well with a theoretical estimation.

[1]H. Cavendish, "Experiments to determine the density of the earth," Philos. Trans. R. Soc. London **88**, 469–526 (1798).

[2]J. H. Gundlach and S. M. Merkowitz, "Measurement of Newton's constant using a torsion balance with angular acceleration feedback," Phys. Rev. Lett. **85**, 2869–2872 (2000).

[3]S. Schlamminger, E. Holzschuh, W. Kündig, F. Nolting, R. E. Pixley, J. Schurr, and U. Straumann, "Measurement of Newton's gravitational constant," Phys. Rev. D **74**(8), 082001 (2006).

[4]H. V. Parks and J. E. Faller, "Simple pendulum determination of the gravitational constant," Phys. Rev. Lett. **105**, 110801 (2010).

[5]R. Davis, "Fundamental constants: Big G revisited," Nature (London) **468**(7321), 181–183 (2010).

[6]See http://www.microglacoste.com/index.html for MicroG-LaCoste, 2013.

[7]J. P. Schwarz, D. S. Robertson, T. M. Niebauer, and J. E. Faller, "A free-fall determination of the newtonian constant of gravity," Science **282**, 2230–2234 (1998).

[8]J. P. Schwarz, D. S. Robertson, T. M. Niebauer, and J. E. Faller, "A new determination of the newtonian constant of gravity using the free fall method," Meas. Sci. Technol. **10**(6), 478 (1999).

[9]G. Lamporesi, A. Bertoldi, L. Cacciapuoti, M. Prevedelli, and G. M. Tino, "Determination of the newtonian gravitational constant using atom interferometry," Phys. Rev. Lett. **100**, 050801 (2008).

[10]T. M. Niebauer, G. S. Sasagawa, J. E. Faller, and F. Klopping, "A new generation of absolute gravimeters," Metrologia **32**, 159–180 (1995).

[11]Ch. Rothleitner, S. Svitlov, H. Mérimèche, H. Hu, and L. J. Wang, "Development of new free-fall absolute gravimeters," Metrologia **46**(3), 283–297 (2009).

[12]B. Hofmann-Wellenhof and H. Moritz, *Physical Geodesy* (Springer Wien, New York, 2005).

[13]2010 CODATA recommended values.

[14]G. Cavagnero, G. Mana, and E. Massa, "Aberration effects in two-beam laser interferometers," J. Opt. Soc. Am. A **23**(8), 1951–1959 (2006).

[15]D. van Westrum and T. M. Niebauer, "The diffraction correction for absolute gravimeters," Metrologia **40**(5), 258–263 (2003).

[16]L. Robertsson, "On the diffraction correction in absolute gravimetry," Metrologia **44**(1), 35 (2007).

[17]Ch. Rothleitner and O. Francis, "Second-order doppler-shift corrections in free-fall absolute gravimeters," Metrologia **48**(3), 187 (2011).

[18]K. Jousten, *Wutz Handbuch Vakuumtechnik* (Vieweg, 2006).

[19]T. M. Niebauer, R. Billson, A. Schiel, D. van Westrum, and F. Klopping, "The self-attraction correction for the FG5X absolute gravity meter," Metrologia **50**(1), 1 (2013).

[20]E. Biolcati, S. Svitlov, and A. Germak, "Self-attraction effect and correction on three absolute gravimeters," Metrologia **49**(4), 560 (2012).

[21]V. Pálinkás, J. Liard, and Z. Jiang, "On the effective position of the free-fall solution and the self-attraction effect of the FG5 gravimeters," Metrologia **49**(4), 552 (2012).

[22]G. D'Agostino, S. Merlet, A. Landragin, and F. Pereira Dos Santos, "Perturbations of the local gravity field due to mass distribution on precise measuring instruments: A numerical method applied to a cold atom gravimeter," Metrologia **48**(5), 299 (2011).

[23]Ch. Rothleitner and O. Francis, "On the influence of the rotation of a corner cube reflector in absolute gravimetry," Metrologia **47**(5), 567–574 (2010).

[24]S. M. Svitlov, C. Rothleitner, and L. J. Wang, "Accuracy assessment of the two-sample zero-crossing detection in a sinusoidal signal," Metrologia **49**, 1–12 (2012).

[25]S. M. Svetlov, "An absolute gravimeter and vibration disturbances: A frequency responses method," in *Gravity, Geoid and Marine Geodesy: International Symposium No. 117, Tokyo, Japan, 30 September–5 October, 1996*, edited by J. Segawa, H. Fujimoto, and S. Okubo (Springer Berlin Heidelberg, 1997), pp. 47–54.

[26]V. D. Nagornyi, "A new approach to absolute gravimeter analysis," Metrologia **32**(3), 201–208 (1995).